

Commensurability Effects at Nonmatching Fields for Vortices in Diluted Periodic Pinning Arrays

C. Reichhardt and C. J. Olson Reichhardt

Theoretical Division, Los Alamos National Laboratory, Los Alamos, New Mexico 87545

(Dated: August 27, 2018)

Using numerical simulations, we demonstrate that superconductors containing periodic pinning arrays which have been diluted through random removal of a fraction of the pins have pronounced commensurability effects at the same magnetic field strength as undiluted pinning arrays. The commensuration can occur at fields significantly higher than the matching field, produces much greater critical current enhancement than a random pinning arrangement due to suppression of vortex channeling, and persists for arrays with up to 90% dilution. These results suggest that diluted periodic pinning arrays may be a promising geometry to increase the critical current in superconductors over a wide magnetic field range.

PACS numbers: 74.25.Qt

I. INTRODUCTION

One of the most important issues for applications of type-II superconductors is achieving the highest possible critical current. This requires preventing the depinning and motion of the superconducting vortices that are present in the sample. A promising approach is the use of artificial pinning arrays, which have been the focus of extensive recent studies. Pinning arrays with triangular, square, and rectangular geometries have been fabricated in superconductors using either microholes or blind holes^{1,2,3,4,5,6} or arrays of magnetic dots^{7,8}. The resulting critical currents are significantly enhanced at the matching magnetic field B_ϕ where the number of vortices equals the number of pinning sites, as well as at higher fields nB_ϕ , with n an integer. At the matching fields, peaks or anomalies in the critical current occur and the vortices form highly ordered commensurate lattices which are free of topological defects^{3,5,6,8,9,10,11,12,13}. Although it might appear that the best method for increasing the overall critical current would be to increase the pinning density and thus increase B_ϕ , this technique fails since adding too many pins to the sample can degrade the overall superconducting properties by lowering T_c and H_{c2} . Thus, an open question is how the critical current can be maximized using the *smallest* possible number of pinning sites. Since completely periodic pinning arrays have been shown to enhance pinning, one can ask whether other pinning arrangements such as quasicrystalline or semiordered arrays could be even more effective at pinning vortices. In recent simulations¹⁴ and experiments^{15,16}, it was demonstrated that a quasicrystalline pinning array produced an enhancement of the critical current compared to a random pinning array for fields below and up to B_ϕ . The enhancement disappears for fields above B_ϕ , however.

In this work we demonstrate a new type of commensurability effect that occurs in periodic pinning arrays that have been diluted by randomly removing a fraction of the pinning sites. In an undiluted array, the commensurability effects occur at fields nB_ϕ . In a diluted array, B_ϕ is reduced; however, the pinning array still retains corre-

lations which are associated with the periodicity of the original undiluted pinning array. In this case, in addition to commensuration effects at B_ϕ , we observe noticeable commensuration effects at the higher field B_ϕ^* , the matching field for the *undiluted* pinning array, even though many of the pins that would have been present in such an array are missing. Strong peaks in the critical current associated with well-ordered vortex configurations appear at nB_ϕ^* . This commensurability effect is remarkably robust and still appears in arrays which have up to 90% of the pinning sites removed, so that $B_\phi^* = 10B_\phi$. In samples with equal numbers of pinning sites, diluted periodic pinning arrays produce considerable enhancement of the critical current for fields well above B_ϕ compared to random pinning arrays. The diluted periodic pinning arrays also have a reduced amount of one-dimensional vortex channeling above B_ϕ compared to undiluted periodic pinning arrays. Such easy vortex channeling is what leads to the reduction of the critical current above B_ϕ in the undiluted arrays. Our results should also apply to related systems such as colloids interacting with periodic substrates¹⁷ and vortices in Bose-Einstein condensates interacting with optical traps¹⁸.

II. SIMULATION

We simulate a two-dimensional system of size $L_x \times L_y$ with periodic boundary conditions in the x and y directions containing N_v vortices and N_p pinning sites. The vortices are modeled as point particles where the dynamics of vortex i is governed by the following equation of motion:

$$\eta \frac{d\mathbf{R}_i}{dt} = \mathbf{F}_i^{vv} + \mathbf{F}_i^{vp} + \mathbf{F}^L. \quad (1)$$

The damping constant $\eta = \phi_0^2 d / 2\pi \xi^2 \rho_N$, where d is the sample thickness, ξ is the coherence length, ρ_N is the normal-state resistivity, and $\phi_0 = h/2e$ is the elementary

flux quantum. The vortex-vortex interaction force is

$$\mathbf{F}_i^{vv} = \sum_{j \neq i}^{N_v} A_v f_0 K_1(R_{ij}/\lambda) \hat{\mathbf{R}}_{ij} \quad (2)$$

where K_1 is the modified Bessel function, A_v is an interaction prefactor which is set to 1 unless otherwise noted, λ is the London penetration depth, $f_0 = \phi_0^2/2\pi\mu_0\lambda^3$, $\mathbf{R}_{i(j)}$ is the position of vortex $i(j)$, $R_{ij} = |\mathbf{R}_i - \mathbf{R}_j|$, and $\hat{\mathbf{R}}_{ij} = (\mathbf{R}_i - \mathbf{R}_j)/R_{ij}$. Forces are measured in units of f_0 and distances in units of λ . The vortex density $B = N_v/L_x L_y$. The vortex-vortex interaction force falls off sufficiently rapidly that a cutoff at $R_{ij} = 6\lambda$ is imposed for computational efficiency and a short range cutoff at $R_{ij} = 0.1\lambda$ is also imposed to avoid a force divergence. The N_p pinning sites are modeled as attractive parabolic potential traps of radius $r_p = 0.2\lambda$ and strength $f_p = 0.25f_0$, with $\mathbf{F}_i^{vp} = (f_p/r_p)R_{ik}\Theta((r_p - R_{ik})/\lambda)\hat{\mathbf{r}}_{ik}^{(p)}$. Here $\mathbf{R}_k^{(p)}$ is the location of pinning site k , $R_{ik} = |\mathbf{R}_i - \mathbf{R}_k^{(p)}|$, $\hat{\mathbf{r}}_{ik}^{(p)} = (\mathbf{R}_i - \mathbf{R}_k^{(p)})/R_{ik}$, and Θ is the Heaviside step function. The pinning density is $B_\phi = N_p/(L_x L_y)$. The pins are placed in a triangular array with matching field B_ϕ^* that has had a fraction P_d of the pins removed, so that $B_\phi = (1 - P_d)B_\phi^*$. The Lorentz driving force $\mathbf{F}^L = F^L \hat{\mathbf{x}}$, assumed uniform on all vortices, is generated by and perpendicular to an externally applied current \mathbf{J} . The initial vortex positions are obtained by simulated annealing from a high temperature. After annealing, the temperature is set to zero and the external drive F^L is applied in increments of $2 \times 10^{-5}f_0$ every 5×10^3 simulation time steps. We measure the average vortex velocity in the direction of the drive, $\langle V \rangle = N_v^{-1} \sum_i^{N_v} \mathbf{v}_i \cdot \hat{\mathbf{x}}$, where \mathbf{v}_i is the velocity of vortex i , and define the critical depinning force f_c as the value of F^L at which $\langle V \rangle = 0.01$. We have found that for slower sweep rates of the driving force, there is no change in the measured depinning force. Finally, we note that our model should be valid for stiff vortices in three-dimensional superconductors interacting with arrays of columnar defects. For a strictly two-dimensional superconductor with periodic pinning arrays the vortex-vortex interaction is modified from a Bessel function to $\ln(r)$; however, our previous simulations have indicated that either interaction produces very similar commensurability effects^{9,10,11,12}.

III. INCREASING DILUTION

A. Fixed Pinning Density

In Fig. 1(a) we illustrate the positions of the pinning sites for an $18\lambda \times 18\lambda$ system with no dilution, $P_d = 0$. The pinning sites are placed in a triangular array at a pinning density of $B_\phi = 0.52/\lambda^2$, giving $B_\phi = B_\phi^* = 0.52/\lambda^2$. Figure 1(b) shows a system with $B_\phi = 0.52/\lambda^2$ and dilution $P_d = 0.5$, so that $B_\phi^* = 1.04/\lambda^2$. Here,

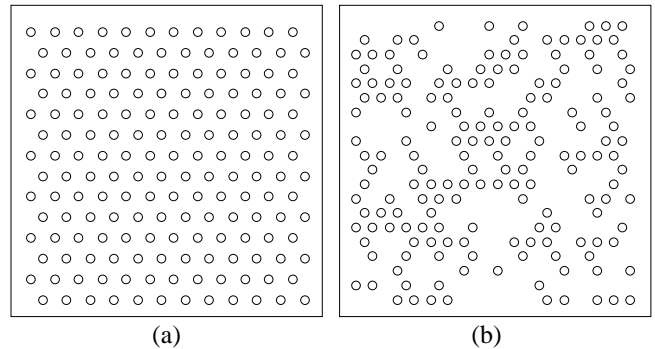


FIG. 1: Circles: Pinning site locations for two $18\lambda \times 18\lambda$ samples with the same number of pinning sites $N_p = 168$. (a) A triangular pinning array with no dilution, $P_d = 0$, with $B_\phi = 0.52/\lambda^2$ and $B_\phi^* = 0.52/\lambda^2$. (b) A triangular pinning array that has been diluted at $P_d = 0.5$, with $B_\phi = 0.52/\lambda^2$ and $B_\phi^* = 1.04/\lambda^2$.

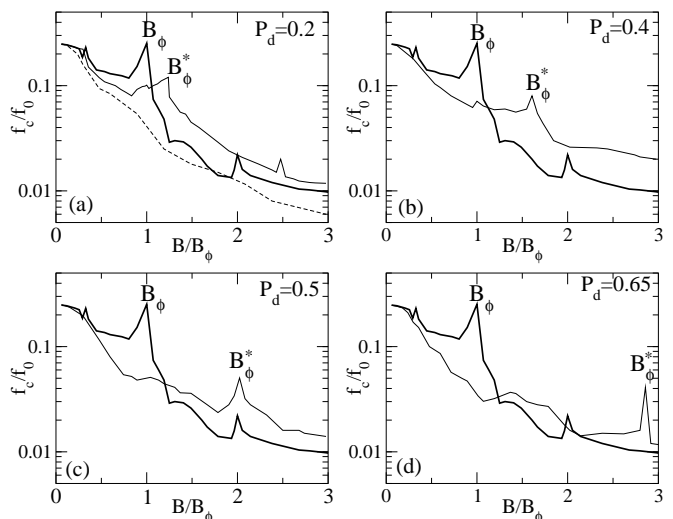


FIG. 2: The critical depinning force f_c/f_0 versus B/B_ϕ for systems with $B_\phi = 0.52/\lambda^2$. The actual matching field B_ϕ and the matching field for an equivalent undiluted array B_ϕ^* are labeled. (a) f_c/f_0 for an undiluted pinning array with $P_d = 0$ (heavy line), a pinning array with $P_d = 0.2$ (light line), and a random pinning arrangement (dashed line). (b) $P_d = 0$ (heavy line) and $P_d = 0.4$ (light line). (c) $P_d = 0$ (heavy line) and $P_d = 0.5$ (light line). (d) $P_d = 0$ (heavy line) and $P_d = 0.65$ (light line).

half of the pinning sites that would have formed a denser triangular array have been removed randomly to give the same matching field B_ϕ as in Fig. 1(a).

To illustrate the effect of the dilution, in Fig. 2(a) we plot the critical depinning force f_c/f_0 vs B/B_ϕ for three systems with $B_\phi = 0.52/\lambda^2$. Two of the samples contain triangular pinning arrays at different dilutions, $P_d = 0$ [as in Fig. 1(a)] and $P_d = 0.2$. The third sample contains randomly placed pinning. For the undiluted triangular pinning array with $P_d = 0$, peaks in the depinning force

occur at integer values of B/B_ϕ . A submatching peak at $B/B_\phi = 1/3$ also appears in agreement with earlier studies¹⁰. The random pinning arrangement shows no commensurability peaks and has a lower critical depinning force than the periodic pinning array for all but the very lowest values of B/B_ϕ . The diluted periodic pinning array has a pronounced peak in f_c/f_0 at $B/B_\phi = 1.25$. This peak corresponds to the matching field B_ϕ^* of the equivalent undiluted pinning array. A second peak in f_c/f_0 occurs at $B = 2B_\phi^*$. There is still a small peak in f_c/f_0 at $B/B_\phi = 1$ for the diluted array; however, we do not find a peak at $B/B_\phi = 2$. The diluted pinning array has a higher f_c/f_0 than both the random pinning arrangement and the undiluted periodic pinning array for $B/B_\phi \gtrsim 1$ over the range of B/B_ϕ investigated here. In most of this range, f_c/f_0 for the diluted periodic array is twice that of the undiluted periodic array.

The peak in f_c/f_0 at $B = B_\phi^*$ persists as the dilution increases. Figure 2(b) shows that a diluted pinning array with $P_d = 0.4$ has a small peak at $B/B_\phi = 1$ and a more prominent peak at $B = B_\phi^*$. The critical depinning force is again higher in the diluted array than in the undiluted array for $B/B_\phi \gtrsim 1.1$. For a diluted pinning array with $P_d = 0.5$, Fig. 2(c) indicates that the commensurability peak in f_c/f_0 has shifted to $B = B_\phi^* = 2B_\phi$. Here, the pinning has become so dilute that there is no longer a noticeable enhancement of f_c/f_0 at $B/B_\phi = 1$. When $P_d = 0.65$, as in Fig. 2(d), the peak in f_c/f_0 shifts up to $B = B_\phi^* = 2.86B_\phi$. As B_ϕ^* increases with increasing dilution, the critical depinning force at lower fields $B < B_\phi^*$ decreases. These results suggest that diluted periodic arrays may be useful for increasing the overall pinning force at higher fields, and that a peak in the critical current at a specific field B_p can be achieved using a *significantly smaller number of pins* than would be required to create an undiluted periodic pinning array with $B_\phi = B_p$.

To understand the origin of the peak in f_c/f_0 at B_ϕ^* , we analyze the vortex configurations at B_ϕ^* for four different values of P_d in Fig. 3. For an undiluted triangular pinning array at $P_d = 0$, as shown in Fig. 3(a), $B_\phi^* = B_\phi$, each pin captures exactly one vortex, and there are no interstitial vortices trapped in the regions between pinning sites. In Fig. 3(b), at $B = B_\phi^* = 1.25B_\phi$ in a system with $P_d = 0.2$, all of the pinning sites are occupied and the excess interstitial vortices sit at the locations of the missing pinning sites, creating a triangular vortex lattice. As P_d increases, the increasing number of interstitial vortices present at $B = B_\phi^*$ continue to occupy the locations of the missing pinning sites. This is illustrated for $P_d = 0.5$ in Fig. 3(c) and $P_d = 0.65$ in Fig. 3(d). The high symmetry of the triangular vortex lattice configuration at the matching field $B = B_\phi^*$ causes the vortex-vortex interactions to cancel, and the depinning force is determined primarily by the maximum force of the pinning sites, f_p . Defects in the vortex lattice appear just above and below $B = B_\phi^*$, creating asymmetrical vortex-vortex interactions. A vortex associated with a defect experiences an extra force contributing to depinning on the order of

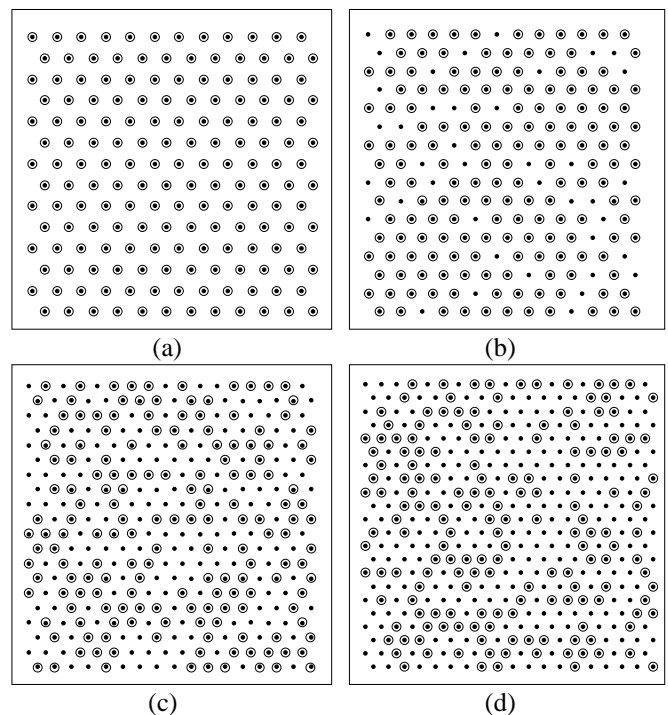


FIG. 3: Positions of pinning sites (open circles) and vortices (black dots) for samples with $B_\phi = 0.52/\lambda^2$ at $B/B_\phi^* = 1$. (a) $P_d = 0$, $B_\phi^* = B_\phi$. (b) $P_d = 0.2$, $B_\phi^* = 1.25B_\phi$. (c) $P_d = 0.5$, $B_\phi^* = 2B_\phi$. (d) $P_d = 0.65$, $B_\phi^* = 2.86B_\phi$.

$F^{vv}(a/\lambda)$, where a is the vortex lattice constant, and f_c is reduced. A similar disordering process occurs just above and below each of the higher matching fields⁹, although in this case the depinning force is not merely determined by the pinning force since a portion of the vortices are pinned indirectly in interstitial positions and experience a weaker effective pinning force.

Previous work on wire network arrays¹⁹ showed that even if the network is partially disordered, spatial correlations remain present as indicated by the appearance of peaks in k -space and can produce matching effects. In the diluted pinning arrays we consider here, even though a portion of the sites are removed there are still peaks in the reciprocal space corresponding to the original undiluted array, so matching effects occur when the vortex lattice k spacing is the same as these pinning array k space peaks. We note that if an equivalent number of randomly placed pinning sites is used there is no matching effect since there is a ring rather than peaks in k space.

In the case of the diluted periodic pinning array, the vortex configuration contains numerous topological defects at $B = B_\phi$ for higher values of P_d when the pinning is strong enough that most of the vortices are trapped at the pinning sites. In contrast, at $B = B_\phi^*$ the vortex lattice is free of defects, as illustrated in Fig. 3. For fields just above or below $B = B_\phi^*$, vacancies and interstitials appear in the vortex lattice and lower the depinning

force. At higher fields $B = nB_\phi^*$, where $n > 1$ is an integer, the vortex lattice is again ordered and a peak in the critical depinning force occurs, as shown in Fig. 2(a) at $B = 2B_\phi^*$.

The enhancement of f_c/f_0 in the diluted periodic pinning arrays for $B/B_\phi > 1$ at the nonmatching fields occurs due to a different mechanism. We first note that at $B/B_\phi < 1$, f_c/f_0 is lower in the diluted pinning arrays than in the undiluted pinning arrays since it is possible for some of the vortices to sit in interstitial sites instead of in pinning sites, even though not all of the pins have been filled. Interstitial vortices experience an effective pinning force due to the interactions with the surrounding vortices. Since the interstitial vortices are more weakly pinned than vortices in pinning sites, the critical depinning force is lower than it would be for an undiluted array at $B/B_\phi < 1$, where every vortex sits in a pinning site. For $B/B_\phi > 1$, the initial motion of the vortices at depinning in an undiluted array occurs via channeling of the interstitial vortices between the pinning sites along an effective modulated one-dimensional potential created by the vortices located at the pinning sites¹¹. In a diluted periodic pinning array at $B_\phi < B < B_\phi^*$, any channels of interstitial vortices are interrupted by one or more pinning sites which serve to increase the depinning threshold of the entire channel by “jamming” free motion along the channel. Here, the one-dimensional potentials that allow for relatively free interstitial vortex motion do not form until $B > B_\phi^*$ when the vortices begin to occupy positions that would be interstitial sites in the equivalent undiluted pinning array. This picture is confirmed by our analysis of the vortex trajectories. The jamming effect eventually breaks down at high dilutions P_d when large regions devoid of pinning sites span the entire system and provide macroscopic channels for free vortex flow. In Fig. 2(d) at $P_d = 0.65$, f_c/f_0 at $B/B_\phi > 1$ is lower than the f_c/f_0 values obtained at lower P_d and similar fields. For higher values of P_d this effect becomes more pronounced until f_c/f_0 eventually drops below the critical depinning current for the undiluted array.

B. Decreasing Pinning Density

In Fig. 4 we show the effect of gradually diluting a periodic pinning array with $B_\phi^* = 0.83/\lambda^2$. The main peak in the critical depinning current always falls at $B = B_\phi^*$, but as the dilution increases from $P_d = 0$ to $P_d = 0.9$, the value of f_c/f_0 decreases significantly. The pronounced peak in f_c/f_0 persists even up to 90% dilution. There is a small peak at $B = B_\phi$ for $P_d = 0.25$, but for higher dilutions we find no noticeable anomalies in f_c/f_0 at $B = B_\phi$. This result indicates that the commensurability effect at $B = B_\phi^*$ is remarkably robust.

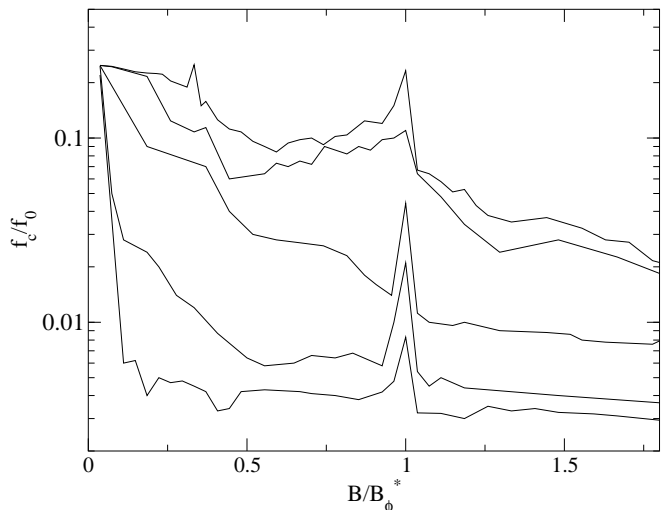


FIG. 4: f_c/f_0 vs B/B_ϕ^* , where $B_\phi^* = 0.83/\lambda^2$. Top curve: an undiluted periodic pinning array with $B_\phi = 0.83/\lambda^2$. Remaining curves, from top to bottom: Successive dilutions of the same array to $P_d = 0.25, 0.5, 0.75$, and 0.9 .

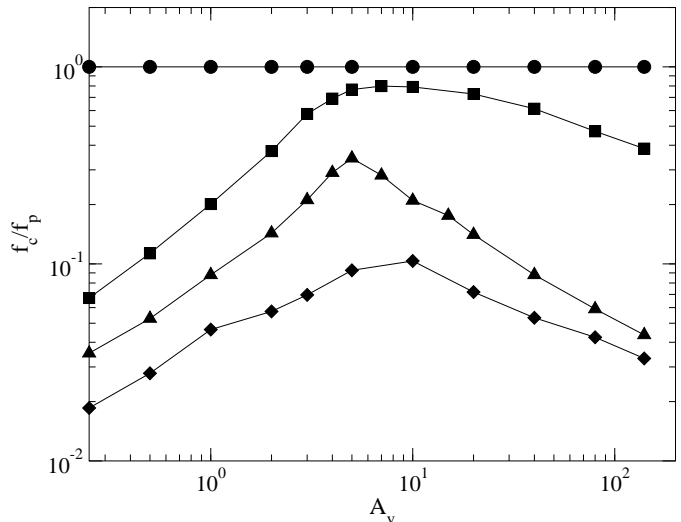


FIG. 5: f_c/f_p vs A_v , the vortex-vortex interaction prefactor, for four samples with $B = 0.52/\lambda^2$. Circles: undiluted triangular array with $B/B_\phi = 1$ and $B_\phi = 0.52/\lambda^2$. Squares: diluted pinning array with $P_d = 0.5$ at $B/B_\phi^* = 1$ where $B_\phi^* = 0.52/\lambda^2$. Triangles: undiluted array with $B/B_\phi = 2.0$ and $B_\phi = 0.26/\lambda^2$. Diamonds: random array with $B/B_\phi = 2.0$ and $B_\phi = 0.26/\lambda^2$.

IV. EFFECT OF VORTEX LATTICE STIFFNESS

We next consider the effect of the vortex lattice stiffness. This parameter can be changed artificially by adjusting the value of the factor A_v in the vortex-vortex interaction term of Eq. (2). For dense random pinning where there are more pinning sites than vortices, $N_p > N_v$, decreasing the strength of the vortex-vortex interactions by lowering A_v makes the vortex lattice softer

and the depinning force increases. In the limit of $A_v = 0$ the vortices respond as independent particles and the depinning force will equal f_p ^{20,21}. In the case where there are more vortices than pinning sites $N_v > N_p$, the situation can be more complicated since there are two types of vortices. One species is located at the pinning sites and the other species is in the interstitial sites. The interstitial vortices are not directly pinned by the pinning sites but are restrained through the vortex-vortex interaction with pinned vortices. In this case it could be expected that increasing the vortex-vortex interactions by raising A_v would increase the depinning force. On the other hand, if the vortex-vortex interaction force is strong enough, the interstitial vortices can more readily push the pinned vortices out of the individual pinning sites. Studies of very diluted random pinning arrays found that as the vortex-vortex interaction is increased, the depinning force initially increases linearly; however, for high enough vortex-vortex interactions the depinning curve begins to decrease again²². The peak in the depinning force coincides with a crossover from plastic depinning at low vortex-vortex interaction strengths to elastic depinning at high vortex-vortex interaction strengths. A similar behavior was observed for vortices in periodic pinning where there were more vortices than pinning sites²¹.

For the results presented in Fig. 2 and Fig. 4, the vortex-vortex interaction prefactor was set to $A_v = 1.0$ and the depinning was plastic with the interstitial vortices depinning first. In Fig. 5 we plot f_c/f_p vs A_v at fixed $B = 0.52/\lambda^2$ for four different pinning geometries. In an undiluted pinning array with $B/B_\phi = 1$, the vortex lattice matches exactly with the pinning array and the vortex-vortex interactions completely cancel. As a result, the system responds like a single particle and $f_c = f_p$ for all A_v , as shown by the circles in Fig. 5. When the same pinning array is diluted to $P_d = 0.5$ and held at $B/B_\phi^* = 1$, the squares in Fig. 5 illustrate that for $0.25 \leq A_v < 5.0$ the depinning is plastic and f_c/f_p linearly increases with A_v . This behavior is agreement with earlier studies^{21,22}. For $A_v > 5.0$ the depinning is elastic and the entire lattice moves as a unit. In this elastic regime f_c/f_p first levels off and then decreases with increasing A_v as the force exerted on the pinned vortices by the interstitial vortices increases. This result indicates that f_c/f_p is maximized at the transition between plastic and elastic depinning. The filled triangles in Fig. 5 show the behavior of an undiluted array at $B/B_\phi = 2$ where the vortex lattice has a honeycomb structure rather than triangular symmetry⁹. Here the f_c/f_p versus A_v curve has a very similar trend to the $P_d = 0.5$ case, with a peak in f_c/f_p at the crossover between plastic and elastic depinning followed by a decrease in the depinning force for $A_v > 5.0$; however, f_c/f_p drops off more quickly for the undiluted pinning array at $B/B_\phi = 2$ than for the diluted pinning array with $P_d = 0.5$. The vortex lattice is always triangular for the $P_d = 0.5$ diluted pinning array at $B/B_\phi^* = 1$, so as A_v increases there is no change in the vortex lattice structure and every pinning site remains

occupied. For the undiluted pinning array at $B/B_\phi = 2$ the vortex lattice experiences an increasing amount of distortion for $A_v > 5.0$ as the structure changes from a honeycomb arrangement in which all of the pinning sites are occupied to a triangular arrangement in which some pins are empty. This implies that for stiff vortex lattices, a relatively larger depinning force can be obtained from a diluted pinning array than from an undiluted pinning array with an equal number of pinning sites. The triangles in Fig. 5 show the behavior of a random pinning array at a pinning density of $B_\phi = 0.26/\lambda^2$ with $B/B_\phi = 2$. We find the same trend of a peak in f_c/f_p as a function of A_v ; however, f_c/f_p for the random pinning array is always less than that of the periodic or diluted pinning arrays. We note that a peak in f_c/f_p still appears for vortex densities that are well away from commensuration due to the competition between the pinning energy and elastic vortex lattice energy.

One aspect we did not explore in this work is the effect of melting and thermal fluctuations on the diluted pinning arrays. Melting would be relevant in strongly layered superconductors with periodic arrays of columnar defects. If a diluted periodic pinning array could be fabricated in a layered superconductor, it is likely that a rich variety of thermally induced effects would appear. One system that should have similar behavior is a sample with a low density of randomly placed columnar defects in which the number of vortices is much greater than the number of pinning sites²³. Theoretical work suggests that such a system can undergo a Bragg-Bose glass transition^{24,25}. In the case where the pinning is periodic, it would be interesting to determine whether the melting transition shifts upward or downward at $B/B_\phi^* = 1$ compared to away from $B/B_\phi^* = 1$. Additionally, at intermediate dilution it may be possible to observe two-stage melting or a nanoliquid. Such a nanoliquid has been observed in experiments with patterned regions of columnar defects²⁶.

V. SUMMARY

In summary, we have demonstrated that commensuration effects can occur in superconductors with diluted periodic pinning arrays. Pronounced peaks in the critical depinning current occur at magnetic fields corresponding to the matching field for the undiluted array, B_ϕ^* , which may be significantly higher than the matching field B_ϕ for the pinning sites that are actually present in the sample. The commensurability effect is associated with the formation of ordered vortex lattice arrangements containing no topological defects. This effect arises since the diluted pinning array has correlations in reciprocal space at the same values of k as the undiluted pinning array, enabling a matching effect to occur for the diluted array when the vortex density matches the density of the undiluted array. The effect is remarkably robust, and peaks in the critical depinning force persist in pinning arrays that have been

diluted up to 90%. For small dilutions, a peak can also appear at the true matching field B_ϕ . In samples with equal numbers of pinning sites, diluted periodic arrays have smaller critical depinning currents than undiluted arrays at fields below B_ϕ , but produce a significant enhancement of the critical current at fields above B_ϕ compared to both undiluted arrays and random pinning arrangements. This enhancement for $B < B_\phi$ is due to the suppression of easy channels of one-dimensional motion that occur in the undiluted arrays. We have also examined the effect of the vortex lattice stiffness on depinning. For $B > B_\phi$, the depinning is plastic in soft lattices and the interstitial vortices begin to move before the pinned vortices, while for stiff lattices the depinning is elastic and the entire lattice depins as a unit. In the plastic depinning regime which appears at small lattice stiffness,

the depinning force increases with increasing lattice stiffness since the interstitial vortices become more strongly caged by the vortices at the pinning sites. In the elastic depinning regime the depinning force decreases with increasing lattice stiffness. A peak in the depinning force occurs at the crossover between plastic and elastic depinning. For stiffer lattices the diluted pinning arrays show more pronounced matching effects. Our results suggest that diluted periodic pinning arrays may be useful for enhancing the critical current at high fields in systems where only a limited number of pinning sites can be introduced.

This work was carried out under the auspices of the NNSA of the U.S. Dept. of Energy at LANL under Contract No. DE-AC52-06NA25396.

-
- ¹ A.T. Fiory, A.F. Hebard, and S. Somekh, *Appl. Phys. Lett.* **32**, 73 (1978).
- ² M. Baert, V.V. Metlushko, R. Jonckheere, V.V. Moshchalkov, and Y. Bruynseraede, *Phys. Rev. Lett.* **74** 3269 (1995); V.V. Moshchalkov, M. Baert, V.V. Metlushko, E. Rosseel, M.J. VanBael, K. Temst, R. Jonckheere, and Y. Bruynseraede, *Phys. Rev. B* **54**, 7385 (1996).
- ³ K. Harada, O. Kamimura, H. Kasai, T. Matsuda, A. Tonomura, and V.V. Moshchalkov, *Science* **274**, 1167 (1996).
- ⁴ V. Metlushko, U. Welp, G.W. Crabtree, R. Osgood, S.D. Bader, L.E. DeLong, Z. Zhang, S.R.J. Brueck, B. Ilic, K. Chung, and P.J. Hesketh, *Phys. Rev. B* **60**, R12585 (1999); U. Welp, X.L. Xiao, V. Novosad, and V.K. Vlasko-Vlasov, *ibid.* **71**, 014505 (2005).
- ⁵ S.B. Field, S.S. James, J. Barentine, V. Metlushko, G. Crabtree, H. Shtrikman, B. Ilic, and S.R.J. Brueck, *Phys. Rev. Lett.* **88**, 067003 (2002); A.N. Grigorenko, S.J. Bending, M.J. Van Bael, M. Lange, V.V. Moshchalkov, H. Fangohr, and P.A.J. de Groot, *ibid.* **90**, 237001 (2003).
- ⁶ G. Karapetrov, J. Fedor, M. Iavarone, D. Rosenmann, and W.K. Kwok, *Phys. Rev. Lett.* **95**, 167002 (2005).
- ⁷ J.I. Martín, M. Vélez, J. Nogués, and I.K. Schuller, *Phys. Rev. Lett.* **79**, 1929 (1997); D.J. Morgan and J.B. Ketterson, *ibid.* **80**, 3614 (1998); M.J. Van Bael, K. Temst, V.V. Moshchalkov, and Y. Bruynseraede, *Phys. Rev. B* **59**, 14674 (1999); J.E. Villegas, E.M. Gonzalez, Z. Sefrioui, J. Santamaria, and J.L. Vicent, *ibid.* **72**, 174512 (2005).
- ⁸ D.J. Priour and H.A. Fertig, *Phys. Rev. Lett.* **93**, 057003 (2004); M.V. Milosevic and F.M. Peeters, *ibid.* **93**, 267006 (2004); Q.H. Chen, G. Teniers, B.B. Jin, and V.V. Moshchalkov, *Phys. Rev. B* **73**, 014506 (2006).
- ⁹ C. Reichhardt, C.J. Olson, and F. Nori, *Phys. Rev. B* **58**, 6534 (1998).
- ¹⁰ C. Reichhardt and N. Grønbech-Jensen, *Phys. Rev. B* **63**, 054510 (2001).
- ¹¹ C. Reichhardt, C.J. Olson and F. Nori, *Phys. Rev. Lett.* **78**, 2648 (1997); C. Reichhardt, G.T. Zimányi, and N. Grønbech-Jensen, *Phys. Rev. B* **64**, 014501 (2001).
- ¹² C.J. Olson Reichhardt, A. Libál, and C. Reichhardt, *Phys. Rev. B* **73**, 184519 (2006).
- ¹³ G.R. Berdiyrov, M.V. Milosevic, and F.M. Peeters, *Phys. Rev. Lett.* **96**, 207001 (2006).
- ¹⁴ V.R. Misko, S. Savel'ev, and F. Nori, *Phys. Rev. Lett.* **95**, 177007 (2005); *Phys. Rev. B* **74**, 024522 (2006).
- ¹⁵ M. Kemmler, C. Gürlich, A. Sterck, H. Pöhler, M. Neuhaus, M. Siegel, R. Kleiner, and D. Koelle, *Phys. Rev. Lett.* **97**, 147003 (2006); A.V. Silhanek, W. Gillijns, V.V. Moshchalkov, B.Y. Zhu, J. Moonens, and L.H.A. Leunissen, *Appl. Phys. Lett.* **89**, 152507 (2006).
- ¹⁶ J.E. Villegas, M.I. Montero, C.-P. Li, and I.K. Schuller, *Phys. Rev. Lett.* **97**, 027002 (2006).
- ¹⁷ P.T. Korda, G.C. Spalding, and D.G. Grier, *Phys. Rev. B* **66**, 024504 (2002); K. Mangold, P. Leiderer, and C. Bechinger, *Phys. Rev. Lett.* **90**, 158302 (2003).
- ¹⁸ H. Pu, L.O. Baksmaty, S. Yi, and N.P. Bigelow, *Phys. Rev. Lett.* **94**, 190401 (2005); J.W. Reijnders and R.A. Duine, *Phys. Rev. A*, **71**, 063607 (2005); S. Tung, V. Schweikhard, and E.A. Cornell, *Phys. Rev. Lett.* **97**, 240402 (2006).
- ¹⁹ A. Behrooz, M.J. Burns, D. Levine, B. Whitehead, and P.M. Chaikin, *Phys. Rev. B* **35**, 8396 (1987).
- ²⁰ C.J. Olson, C. Reichhardt, and F. Nori, *Phys. Rev. Lett.* **81**, 3757 (1998); C.J. Olson, C. Reichhardt, and S. Bhattacharya, *Phys. Rev. B* **64**, 024518 (2001).
- ²¹ C. Reichhardt, K. Moon, R. Scalettar, and G. Zimányi, *Phys. Rev. Lett.* **83**, 2282 (1999).
- ²² M.-C. Cha and H.A. Fertig, *Phys. Rev. Lett.* **80**, 3851 (1998).
- ²³ M. Menghini, Y. Fasano, F. de la Cruz, S.S. Banerjee, Y. Myasoedov, E. Zeldov, C.J. van der Beek, M. Konczykowski, and T. Tamegai, *Phys. Rev. Lett.* **90**, 147001 (2003).
- ²⁴ C. Dasgupta and O.T. Valls, *Phys. Rev. Lett.* **91**, 127002 (2003).
- ²⁵ C. Dasgupta and O.T. Valls, *Phys. Rev. B* **69**, 214520 (2004).
- ²⁶ S.S. Banerjee, A. Soibel, Y. Myasoedov, M. Rappaport, E. Zeldov, M. Menghini, Y. Fasano, F. de la Cruz, C.J. van der Beek, M. Konczykowski, and T. Tamegai, *Phys. Rev. Lett.* **90**, 087004 (2003).